

Supporting Information for:

Multinuclear Magnetic Resonance Tracking of Hydro, Thermal and Hydrothermal Decomposition of $\text{CH}_3\text{NH}_3\text{PbI}_3$

Abdelrahman M. Askar,^{1†} Guy M. Bernard,^{2†} Benjamin Wiltshire,¹ Karthik Shankar^{1,3} and
Vladimir K. Michaelis^{2*}

- 1- Department of Chemistry, University of Alberta, Edmonton, Alberta, Canada, T6G 2G2
- 2- Department of Electrical Engineering, University of Alberta, Edmonton, Alberta, Canada, T6G 1H9
- 3- NRC National Institute for Nanotechnology, Edmonton, Alberta, Canada, T6G 2M9

* Corresponding author: vladimir.michaelis@ualberta.ca

Table S1. Crystal Structure Parameters and Pb Coordination for MAPbI₃ and its Decomposition Products.

	MAPbI₃^a	MAPbI₃^a	Monohydrate	Dihydrate	PbI₂
Structure	Cubic	Tetragonal	Monoclinic	Monoclinic	Trigonal
T/K	352	253	100	103	NA
Space Group	<i>Pm-3m</i>	<i>I4/mcm</i>	<i>P2₁/m</i>	<i>P2₁/n</i>	<i>P-3m1</i>
<i>a</i> /Å	6.31728	8.8392	10.469	10.421	4.59
<i>b</i> /Å	6.31728	8.8392	4.6557	11.334	4.59
<i>c</i> /Å	6.31728	12.6948	11.214	10.668	6.78
<i>β</i> /°	90.00	90.00	101.251	91.73	90
<i>Z</i>	1	4	2	2	1
Pb-I/Å (range)	3.1586	3.1736 – 3.1737	3.0637 – 3.3972	3.195 – 3.231	2.977
I-Pb-I/° (range)	90	90	87.352 – 93.009	87.57 – 91.30	100.9
Reference	1	2	3	4	5

- a. MAPbI₃ may also be found in three phases, orthorhombic below 162.7 K, tetragonal between 162.7 and 326.6 K, or in the cubic phase, above 326.6 K.⁶ Data for the latter two phases are given here.

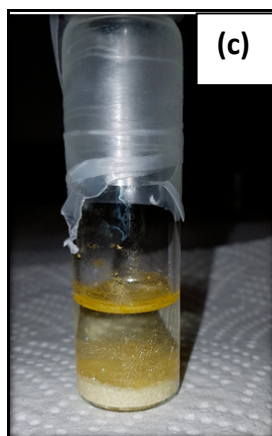
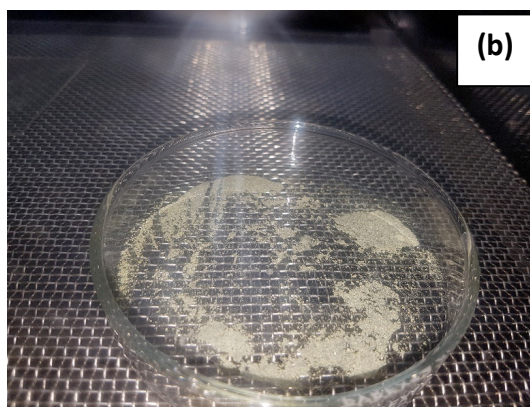
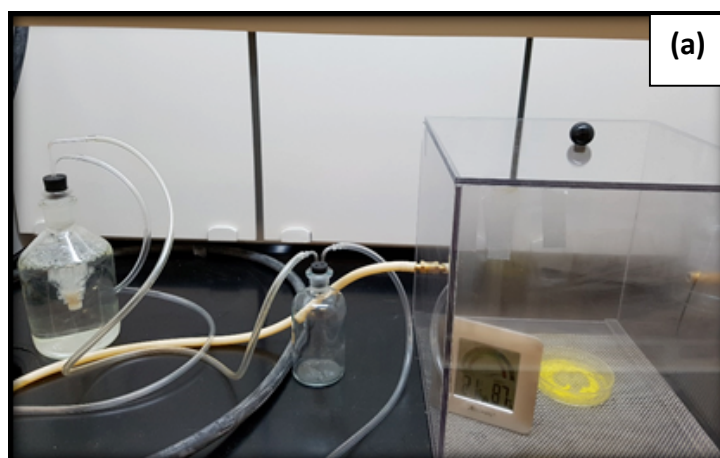


Figure S1: (a) Flow cell apparatus used to control the relative humidity for the various treatments with MAPbI_3 . The yellow powder in the petri dish is the product of MAPbI_3 following prolonged exposure to humidity. (b) Image of MAPbI_3 powder sample after seven days in the humidity cell (RH = 80%, T = 294 K). (c) Image of as-prepared monohydrate sample prior to vacuum drying step.

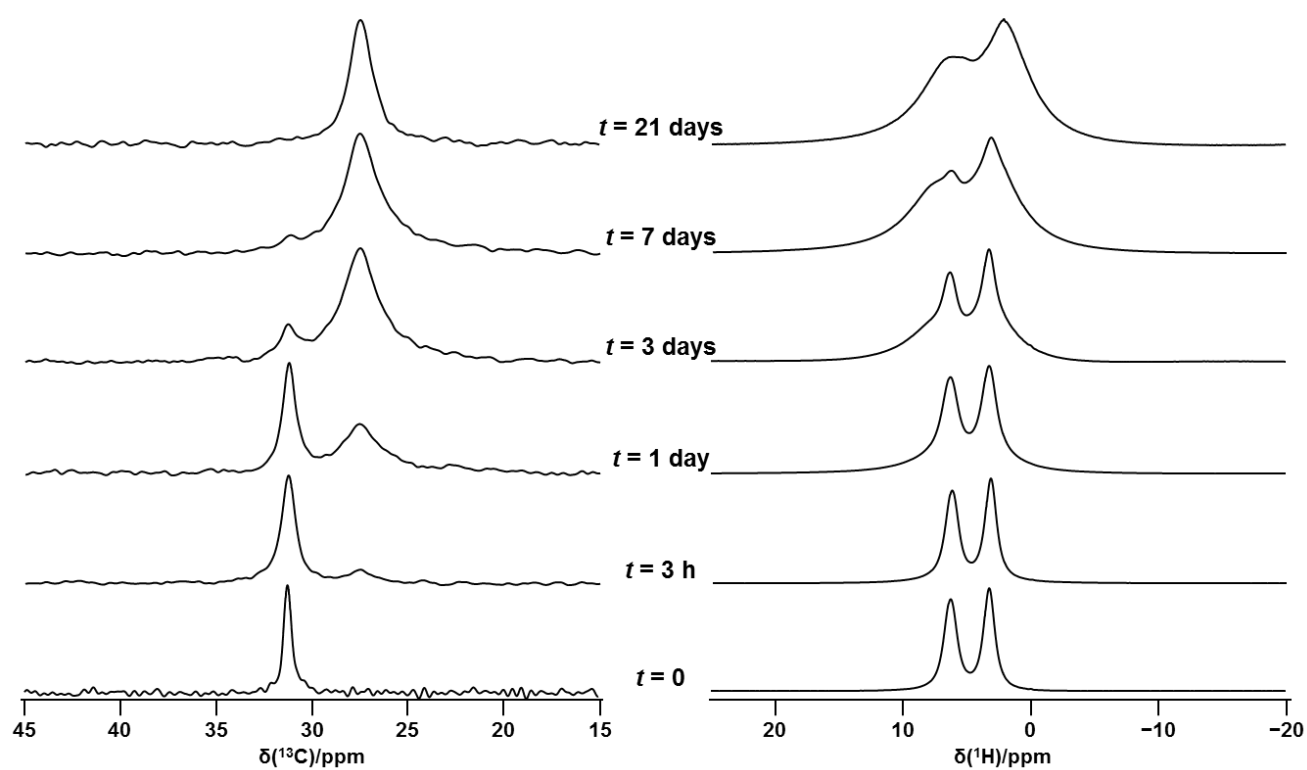


Figure S2: ^{13}C (left) and ^1H (right) MAS NMR spectra of $\text{CH}_3\text{NH}_3\text{PbI}_3$ exposed to 80 % RH for the indicated times. Spectra were acquired at 294 K at 7.05 T (300 MHz ^1H) with a spinning frequency of 5 kHz for the ^{13}C spectra and 12 kHz for the ^1H spectra.

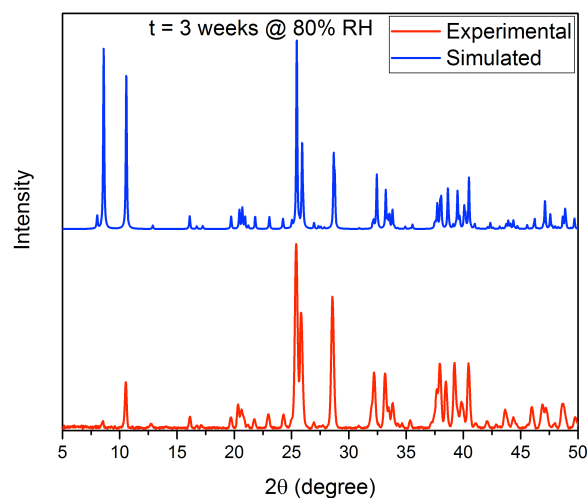


Figure S3: XRD pattern of MAPbI_3 placed in the humidity cell at 80% RH for 3 weeks and simulated pattern of the monohydrate. The simulated pattern is based on the reported single-crystal data (Imler, G. H.; Li, X.; Xu, B.; Dobereiner, G. E.; Dai, H.-L.; Rao, Y.; Wayland, B. B. *Chem. Comm.* 2015, 51, 11290).

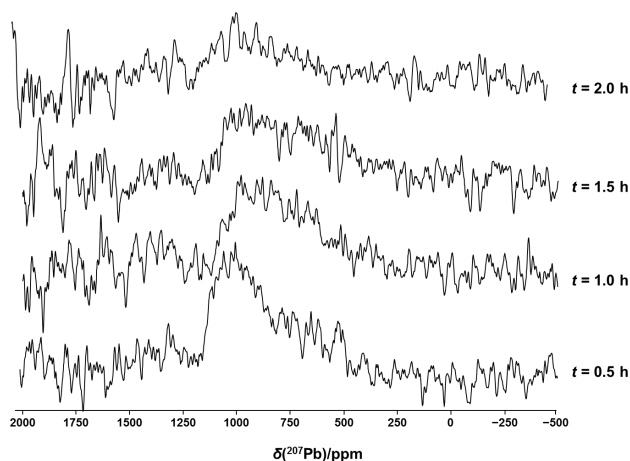


Figure S4: ^{207}Pb NMR spectra of $\text{MAPbI}_3 \cdot \text{H}_2\text{O}$, acquired at 11.75 T at 324 K. A total of 360 transients with a recycle delay of 5 s were used to acquire each spectrum. The times on the right indicate the time after the temperature was initially achieved. The higher noise in the 1500 to 2000 ppm range is attributed to interference from a local FM radio station (see Experimental Section of the manuscript).

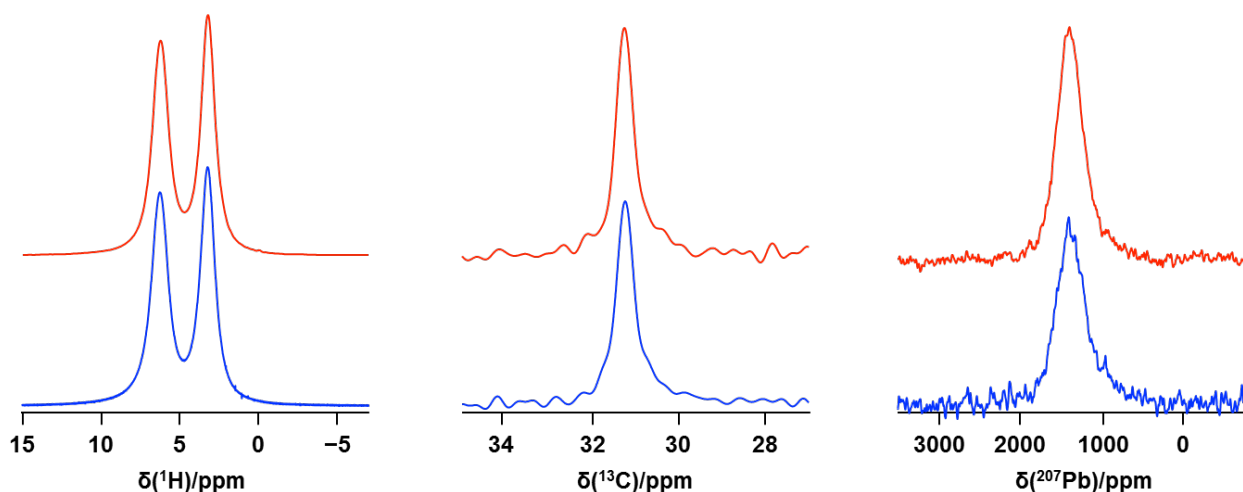


Figure S5. Comparison of ^1H , ^{13}C and ^{207}Pb NMR spectra for MAPbI₃ (upper traces, red) and of the sample after it was subjected to 7 days at 80 % RH, then heated to 341 K (lower traces, blue). Spectra were acquired at 7.05 T at 294 K, with a spinning frequency of 12 kHz (^1H), 5 kHz (^{13}C) or 0 kHz (^{207}Pb).

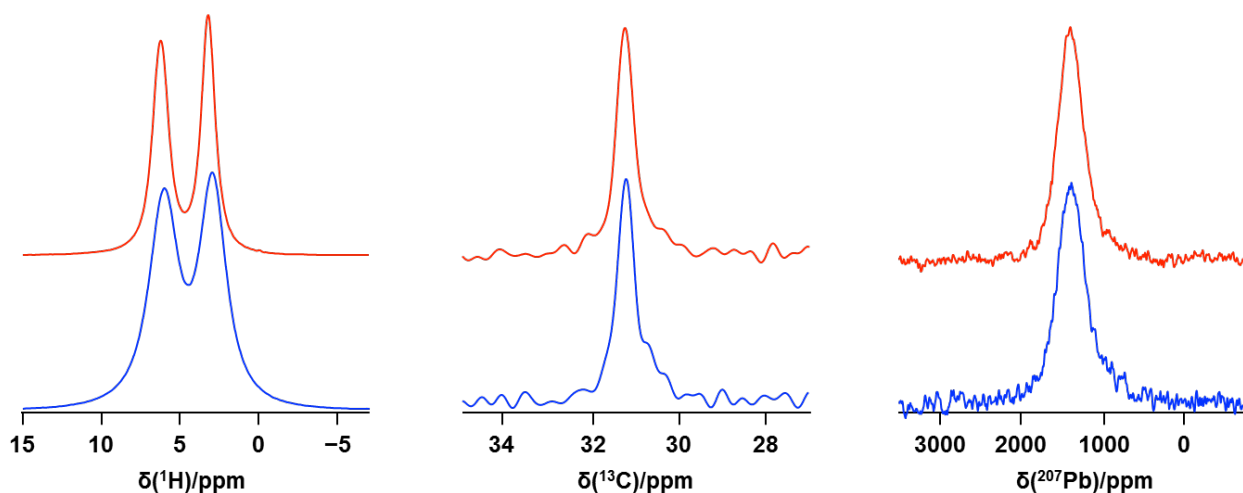


Figure S6. Comparison of ^1H , ^{13}C and ^{207}Pb NMR spectra for MAPbI₃ (upper traces, red) and of the sample after it was subjected to 11 days at 40 % RH (lower traces, blue). Spectra were acquired at 7.05 T at 294 K, with a spinning frequency of 12 kHz (^1H), 5 kHz (^{13}C) or 0 kHz (^{207}Pb).

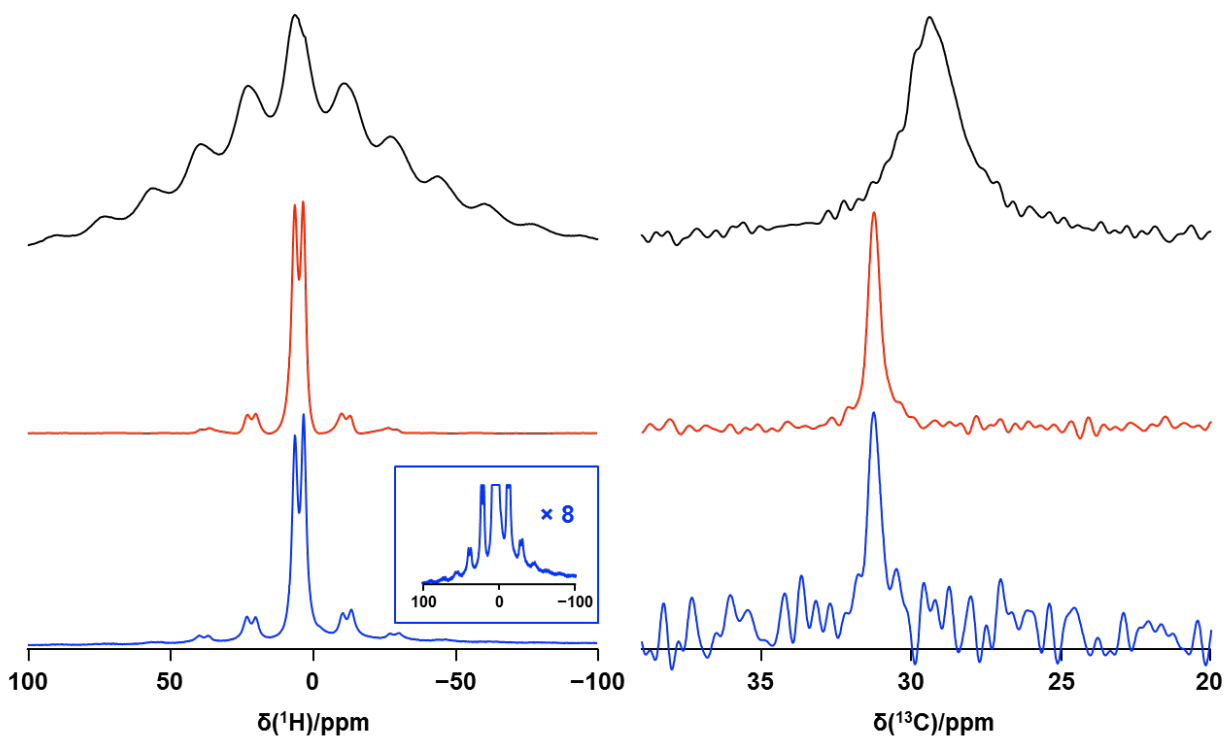


Figure S7. Comparison of ^1H and ^{13}C MAS NMR spectra for MAI (upper traces, black), MAPbI_3 (middle traces, red) and of the sample following the addition of $200\ \mu\text{L H}_2\text{O}(l)$ (lower traces, blue). The inset shows the ^1H spectrum of the latter with its vertical scale multiplied by 8. Spectra were acquired at 7.05 T at 294 K, with a spinning frequency of 5 kHz.

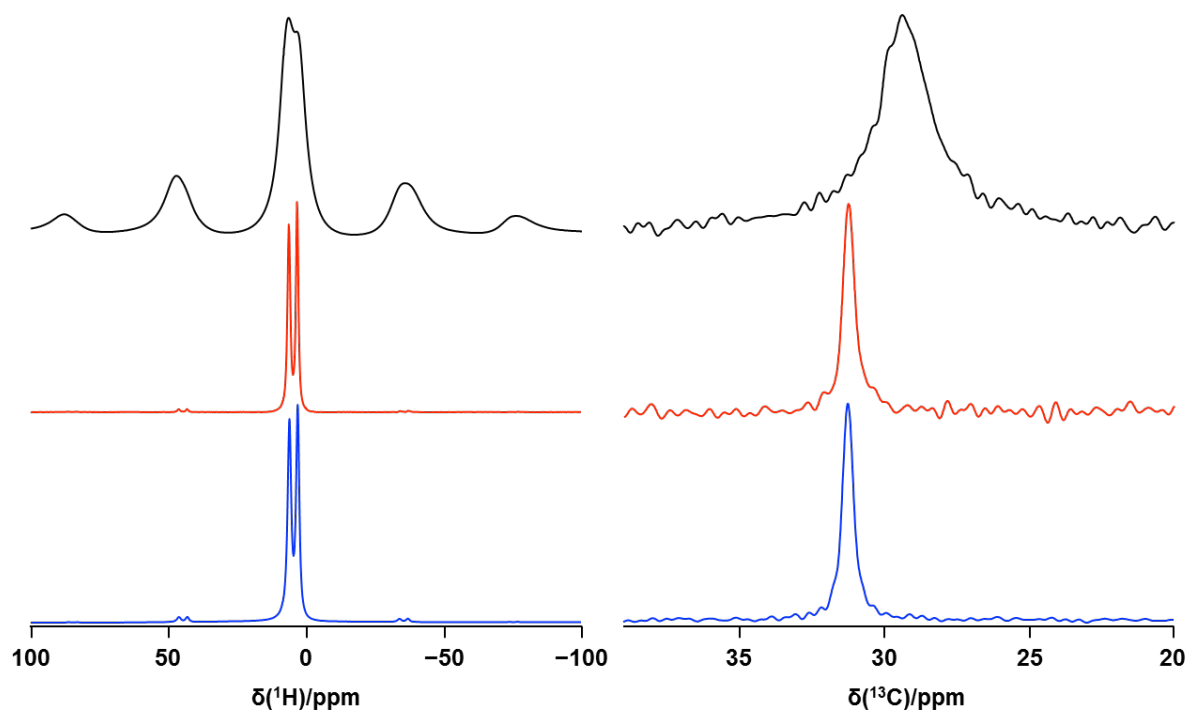


Figure S8. Comparison of ^1H and ^{13}C MAS NMR spectra for MAI (upper traces, black), MAPbI_3 (middle traces, red) and of the sample after it was subjected to 8 days at 45 % RH at $T = 358\text{ K}$ (lower traces, blue). Spectra were acquired at 7.05 T at 294 K, with a spinning frequency of 12 kHz for ^1H and 5 kHz for ^{13}C .

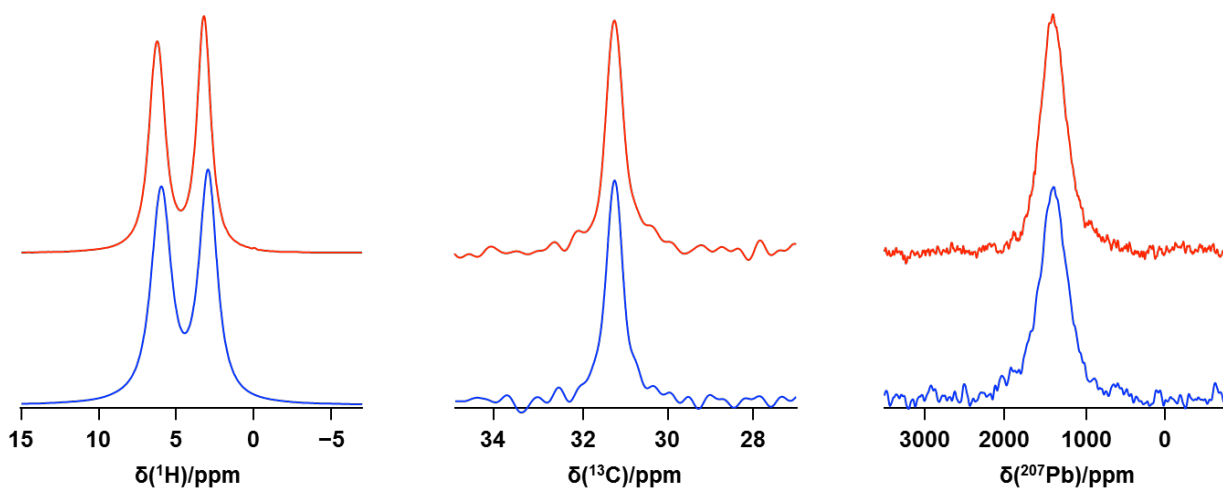


Figure S9. Comparison of ^1H , ^{13}C and ^{207}Pb NMR spectra for MAPbI_3 (upper traces, red) and of the sample after it was left in a furnace for 4 days at 378 K (lower traces, blue). Spectra were acquired at 7.05 T at 294 K, with a spinning frequency of 12 kHz (^1H), 5 kHz (^{13}C) or 0 kHz (^{207}Pb).

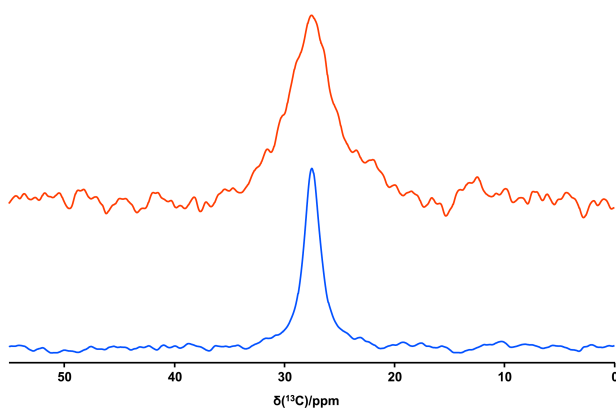


Figure S10. Comparison of ^{13}C NMR spectra for the synthesised monohydrate (upper trace, red) and the slowly annealed 21-day monohydrate (lower trace, blue) within the humidifying chamber (MAPbI_3 at $t=0$ converting to highly crystalline monohydrate, $t=21$ days). Spectra were acquired at 7.05 T at 294 K, with a spinning frequency of 5 kHz (^{13}C).

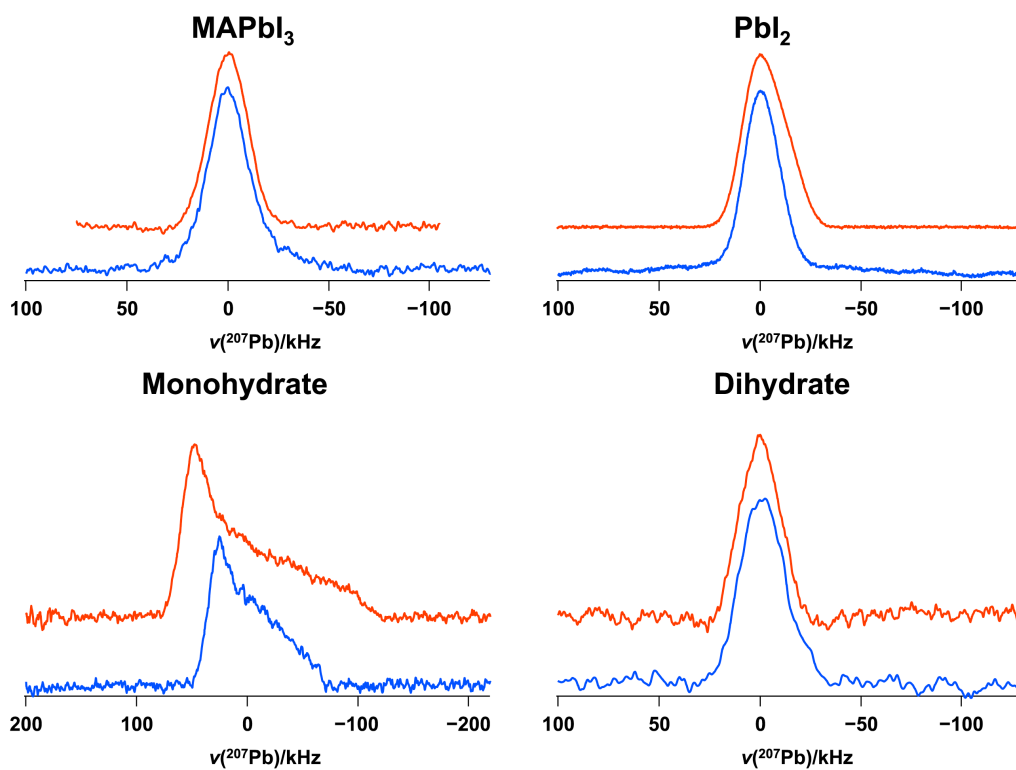


Figure S11. ^{207}Pb NMR spectra of stationary samples of MAPbI_3 , the monohydrate, the dihydrate and PbI_2 , acquired at 11.75 T (upper traces, red) and 7.05 T (lower traces, blue) at 294 K. To facilitate comparisons, the center-of-mass chemical shifts were set to 0.0 kHz for all spectra; see Table 1 in the manuscript for their actual values.

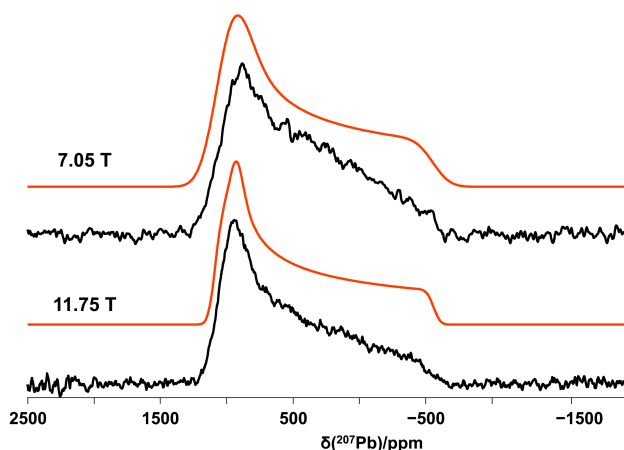


Figure S12. Simulated (red) and experimental (black) ^{207}Pb VOCS of the monohydrate obtained at 7.05 and 11.75 T. Spectra were simulated with $\delta_{\text{iso}} = 485$ ppm, $\Omega = 1650$ ppm and $\kappa = 0.8$.

References:

- ¹ Weller, M.T.; Weber, O.J.; Henry, P.F.; Di Pumpo A.M.; Hansen, T.C. *Chem. Commun.* **2015**, *51*, 4180.
- ² Yamada, Y.; Yamada, T.; Phuong, L. Q.; Maruyama, N.; Nishimura, H.; Wakamiya, A.; Murata, Y.; Kanemitsu, Y. *J. Am. Chem. Soc.* **2015**, *137*, 10456–10459.
- ³ Imler, G.H.; Li, X.; Xu, B.; Dobereiner, G.E.; Dai, H.-L.; Rao, Y.; Wayland, B.B. *Chem. Commun.* **2015**, *51*, 11290–11292.
- ⁴ Wakamiya, A.; Endo, M.; Sasamori, T.; Tokitoh, N.; Ogomi, Y.; Hayase S.; Murata, Y. *Chem. Lett.* **2014**, *43*, 711.
- ⁵ PDF 00-007-0235.
- ⁶ (a) Knop, O.; Wasylishen, R.E.; White, M.A.; Cameron, T.S.; Van Oort, M.J.M. *Can. J. Chem.*, **1990**, *68*, 412. (b) Onoda-Yamamuro, N.; Matsuo, T; Suga, H. *J. Phys. Chem. Solids*, **1990**, *51*, 1383-1395.